

Pyramid-like Gold Electrodeposit Formation in the Stranski-Krastanov Mode

M. Saitou

Department of Mechanical Systems Engineering, University of the Ryukyus, 1 Senbaru Nishihara-cho Okinawa, 903-0213, Japan

E-mail: saitou@tec.u-ryukyu.ac.jp

Received: 10 January 2017 / *Accepted:* 8 February 2017 / *Published:* 12 March 2017

The Stranski-Krastanov (S-K) mode transition in gold electrodeposition using a sodium disulfiteaurate (I) solution was investigated. After a smooth gold thin film was grown on an Indium Tin Oxide (ITO) glass, a pyramid-like gold electrodeposit emerged on the smooth gold thin film. The pyramid-like gold electrodeposit showed a truncated pyramid-like configuration comprising four (111) planes. A critical film thickness at which the pyramid-like gold electrodeposit appears was found to be dependent on temperature. Texture coefficients of the gold thin film determined by x-ray diffraction (XRD) reveal that the S-K mode transition takes place when the (110) plane becomes dominant among the other crystallographic planes such as the (111), the (100), and the (311) plane. A scanning electron microscope (SEM) image shows that the pyramid-like gold electrodeposit formed at the critical film thickness may become a candidate for quantum dots.

Keywords: Stranski-Krastanov mode, pyramid-like gold electrodeposit, critical film thickness, texture coefficient, sodium disulfiteaurate (I)

1. INTRODUCTION

Gold nanomaterials have recently attracted researchers in science and technology because of new quantum effects beyond classical properties of gold, and their applications in a wide field of optoelectronics, biophysics, biochemistry, and biomedical science [1-4]. For example, the coupling of the light wave with surface plasmons of the gold nanomaterial is known as the surface plasmon resonance (SSR). As the SSR signal also gives an information on a molecular interaction absorbed on the gold surface, it is possible to study an interaction between the molecular and gold surface in real time.

The S-K mode has a practical importance owing to an assembly configuration as a device composing quantum dots on a planar film [5]. The mechanism of why the S-K mode that indicates a transition from the two-dimensional growth (layer by layer growth) to the three-dimensional growth occurs in film growth has been experimentally and theoretically investigated [6-8]. When the film with a smooth surface generated by the layer by layer growth reaches a critical film thickness, the S-K mode transition takes place. The critical film thickness in vapor phase epitaxy is usually several monolayers. The three-dimensional deposit formed at the S-K mode transition had no facet. For example, gold clusters generated on the gold smooth film were observed to change a three-dimensional gold island beyond the critical film thickness [9-10].

On the other hand, electrodeposition is a simple and useful technique to synthesize the gold nanoparticles [11-14]. The three-dimensional electrodeposit generated on the smooth gold layer had no facet as well as that in vapor phase epitaxy and showed a plane-like configuration [15]. However, if the nano-electrodeposit is composed of crystallographic planes, it is expected to become a promised material.

In the previous study [16], we reported the formation of pyramid-like electrodeposits comprising four (111) planes in gold electrodeposition. The pyramid-like electrodeposit in the order of submicron meter were generated on the smooth gold film grown on an ITO glass, however, whether or not the growth mode of the pyramid-like electrodeposit obeyed the S-K mode did not make clear.

In the present study, we demonstrate the pyramid-like gold electrodeposit generated at the S-K mode transition and the temperature-dependence of the critical film thickness when the S-K mode takes place.

2. EXPERIMENTAL SET UP

2.1 Gold thin film electrodeposition

An ITO glass of 15x10 mm² and a carbon plate of 35x40 mm² were prepared for a cathode and an anode electrode. An electrochemical cell containing a 0.3 mol/L solution of sodium disulfiteaurate (I) (AuNa₃O₃S₂) was held in electrodeposition in a temperature range from 303 to 323 K.

A rectangular pulse voltage was supplied in electrodeposition with a function generator. A metal film resistor of 22 Ω was connected in series with the electrochemical cell to calculate a rectangular pulse current flowing in the electrochemical cell from a voltage drop between the metal film resistor. In the gold electrodeposition, a frequency of 1 MHz and a rectangular pulse current amplitude (current density) of 22.4 mA/cm² was employed. The current on-time in the rectangular pulse current was chosen to be equal to the current off-time.

After electrodeposition, the gold thin film generated on the ITO glass was rinsed with distilled water and dried. The gold thin film was weighted to the precision of 0.1 mg with an electric balance (AND HR-60). The film thickness was calculated using the weight and the deposited area. The gold thin film on the ITO glass was investigated with SEM (Hitachi TM3030) and XRD (Rigaku Ultima).

The conventional XRD with $\text{CuK}\alpha$ radiation and a standard θ - 2θ diffractometer with a monochromator of carbon was used to determine the crystallographic planes in the gold electrodeposit.

2.2 Internal stress measurement

To measure the internal stress in the gold thin film generated on the ITO glass is a first step to estimate the strain energy that increases with the film thickness. In this study, instead of the ITO glass, a beryllium-copper plate consisting of two legs (Specialty Testing and Development Co. made) was employed to measure the internal stress, which is known as the bent strip measurement [17]. The strain across the interface between the beryllium copper plate and the gold thin film may be different from that between the ITO glass and the gold thin film. Hence, the strain measured by the bent strip technique may be regarded as the first order of approximation. Two carbon sheets of $90 \times 60 \times 0.5 \text{ mm}^3$ were prepared for the anode electrodes. The gold electrodeposition on the bent strip using the solution was performed at a frequency of 1 MHz, a temperature of 303 K, and a current density of 22.4 mA/cm^2 .

3. RESULTS AND DISCUSSION

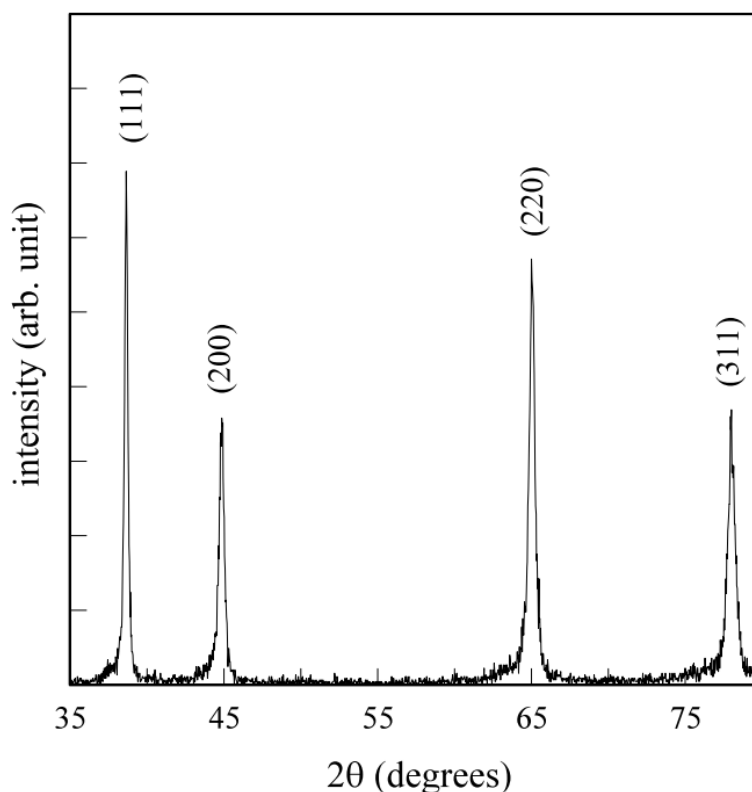


Figure 1. XRD chart of the gold thin film generated at a current density of 22.4 mA/cm^2 , a frequency of 1 MHz, a temperature of 313 K. The gold thin film had $2.0 \mu\text{m}$ in thickness.

Figure 1 shows a typical XRD chart of the gold thin film generated at a temperature of 313 K, a

current density of 22.4 mA/cm^2 , and a frequency of 1 MHz. The gold thin film had $2.0 \mu\text{m}$ in thickness and appeared mirror-like. Diffraction peaks by the crystallographic plane such as the (111), the (200), the (220), and the (311) plane in Fig.1 are well consistent with those of polycrystalline gold [18]. Peaks diffracted by materials other than gold were not found. The mean grain size determined by the Scherrer equation was about 30 nm. The diffraction peak of the (220) plane, which is not normalized, is intense in comparison with that of the (111) plane. The ratio of the (110) plane in the gold thin film parallel to the ITO substrate is expected to be large.

Thus, the thin film on which the pyramid-like electrodeposit was generated is shown to be composed of only gold [16].

3.1 Pyramid-like gold electrodeposit in the S-K mode

The critical film thickness in vapor phase epitaxy is reported to depend on the deposition temperature [6]. An increase in the deposition temperature monotonously lessens the critical film thickness. An increase in the entropy by temperature is understood to cause a decrease in the critical film thickness. The value of the critical film thickness in vapor phase epitaxy is about several monolayers.

The temperature-dependence of the critical film thickness in electrodeposition has not been reported as far as we know. In addition, the three-dimensional grain formed at the S-K transition in vapor phase epitaxy is different in that the electrodeposit formed on the smooth layer has a symmetrical property such as the pyramid-like shape. Hence, the critical film thickness in electrodeposition may not simply decrease with temperature.

3.1.1 Pyramid-like electrodeposit at 303 K

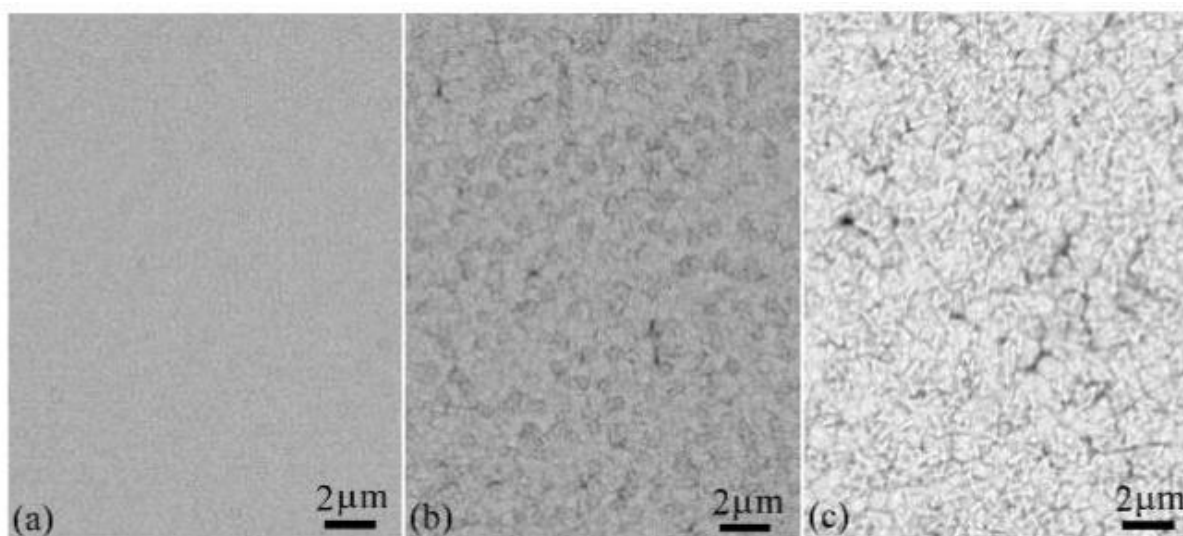


Figure 2. SEM images of the gold thin film having a film thickness of (a) $0.81 \mu\text{m}$, (b) $0.95 \mu\text{m}$, and (c) $1.4 \mu\text{m}$. The gold electrodeposits were generated at a solution temperature of 303 K and a current density of 22.4 mA/cm^2 .

Figure 2 shows SEM images of the gold thin film generated at a temperature of 303 K. The snapshots demonstrate the presence of the critical film thickness. The gold thin film of 0.81 μm in thickness appears smooth in Fig. 2 (a). The pyramid-like electrodeposit emerges on the smooth gold thin film of 0.95 μm in thickness in Fig. 2 (b). The S-K mode transition takes place in the gold thin film growth. As reported [16], the pyramid-like electrodeposit is composed of four triangular (111) planes and one square (110) plane. This is different from the grains observed in vapor phase epitaxy. The pyramid-like electrodeposit has a high symmetrical property.

The formation of a gold nanowire with the tip of the pyramid-like configuration was reported using a vapor phase epitaxy technique [19]. The nanowire was grown on a gold nano-seed and had a growth direction of $\langle 110 \rangle$. The nanowire was shown to have the facets at a nanometer level.

In order to investigate a relationship between the appearance of the S-K mode and crystallographic planes in the gold film, XRD was employed. The texture coefficient [16] $T(hkl)$ is calculated using the following equation defined by

$$T(hkl) = \frac{I(hkl)_i / I_o(hkl)_i}{\sum_N I(hkl)_i / I_o(hkl)_i}, \tag{1}$$

where $I(hkl)_i$ is the measured intensity of the (hkl) diffraction, $I_o(hkl)_i$ is the standard intensity of polycrystalline gold [18], and N is the total number of a diffraction peak.

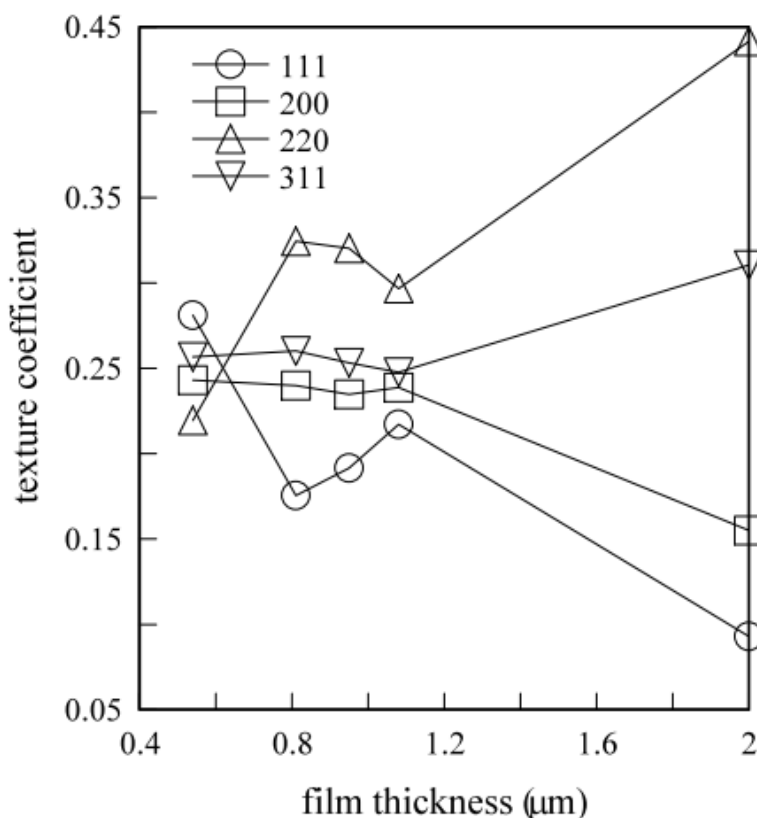


Figure 3. A plot of the texture coefficient vs. the film thickness. The gold thin films were generated at a solution temperature of 303 K, a current density of 22.4 mA/cm².

Figure 3 shows the texture coefficient dependent on the film thickness. The texture coefficient indicates the ratio of the presence of the crystallographic plane in the gold thin film. The four planes such as the (111) plane, the (200) plane, the (220) plane, and the (311) plane coexist at the initial stage. However, when the film growth proceeds, the instability of the ratio among the four planes occurs. That is, a texture change between the (220) plane and the three planes starts at about 0.64 μm . The (220) and the (311) plane become dominant at a film thickness above 0.95 μm .

The (110) plane has the largest surface energy among the (111), the (100) and the (110) plane [20]. In addition, the (110) plane has the largest exchange current density among the (111), the (100), and the (110) plane [21]. In electrodeposition, the crystallographic plane with the largest exchange current density rather than the smallest surface energy often emerges [16] when a high current density is applied in electrodeposition. In this study, the (110) and the (311) plane become dominant. In the theoretical framework of the S-K mode [6], the free energy of the thin film comprises the binding energy, the strain energy, and the entropy. The binding energy is divided into the surface energy and edge (step) energy. The (110) and the (311) plane increase the free energy owing to an increase in the ratio with the film thickness. Hence, the S-K mode transition may occur to lessen the free energy because the (111) plane of the pyramid-like electrodeposit has the smallest surface energy.

3.1.2 Pyramid-like electrodeposit at 313 K

Figure 4 shows snapshots of SEM images that indicate the appearance of the pyramid-like gold electrodeposit. The gold thin film of 0.41 μm in thickness appears smooth in Fig. 4 (a).

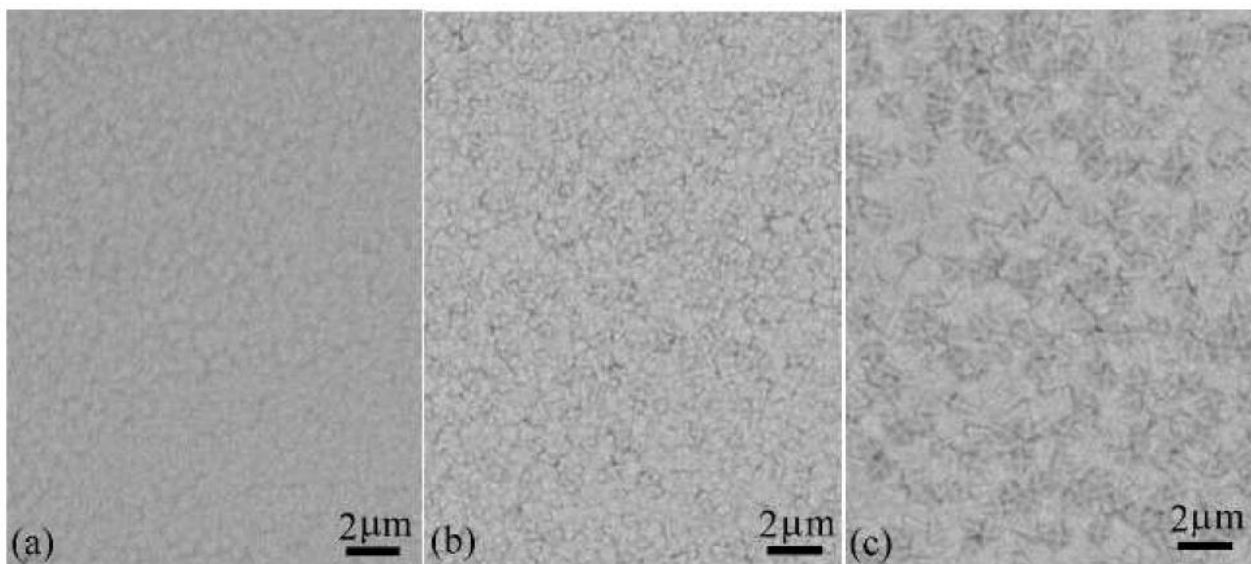


Figure 4. SEM images of the gold thin film having a film thickness of (a) 0.41 μm , (b) 0.54 μm , and (c) 1.35 μm . The gold electrodeposits were generated at a solution temperature of 313 K and at a rectangular pulse current amplitude of 22.4 mA/cm^2 .

The pyramid electrodeposit emerges on the gold thin film of 0.54 μm in Fig. 4 (b). The S-K mode transition takes place in the gold thin film growth. The critical film thickness decreases in

comparison with that at 303 K, which is consistent with experimental results in vapor phase epitaxy [5]. The pyramid-like deposit was observed in the study using an electroless deposition technique [22]. However, the formation in a solution did not follow the S-K mode transition. The four facets were inferred to be triangular (111) planes owing the interior angle between the intersection edges of the triangles.

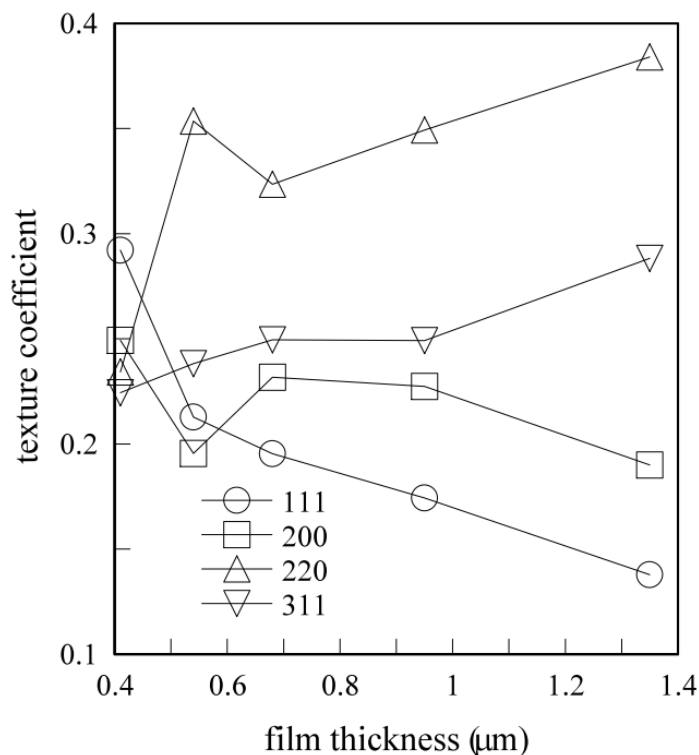


Figure 5. A plot of the texture coefficient vs. the film thickness. The gold thin films were generated at a solution temperature of 313 K, a current density of 22.4 mA/cm².

Figure 5 shows a plot of the texture coefficient vs. the film thickness. The texture change between the (220) plane and the (111) plane occurs at a film thickness of 0.45 μm. The texture change between the (311) plane and the (111) plane also occurs at a film thickness of 0.52 μm. These texture changes start at a thinner film thickness than that in Fig. 3. The ratios of the (100) and the (111) plane decrease with the film thickness.

3.1.3 Pyramid-like electrodeposit at 323 K

Figure 6 shows snapshots of SEM images that indicate the appearance of the pyramid-like gold electrodeposit. The gold thin film of 0.9 μm in thickness has a smooth surface in Fig. 6 (a). The gold thin film obeys the two-dimensional growth (layer by layer). The pyramid electrodeposit emerges on the gold thin film of 1.1 μm in Fig. 6. (b). The growth mode of the gold thin film changes in the three-dimensional growth. The S-K mode transition is shown to take place in the gold thin film growth. The critical film thickness increases in comparison with that at 313 K. This is different from the temperature-dependence of the critical film thickness in vapor phase epitaxy [6-7].

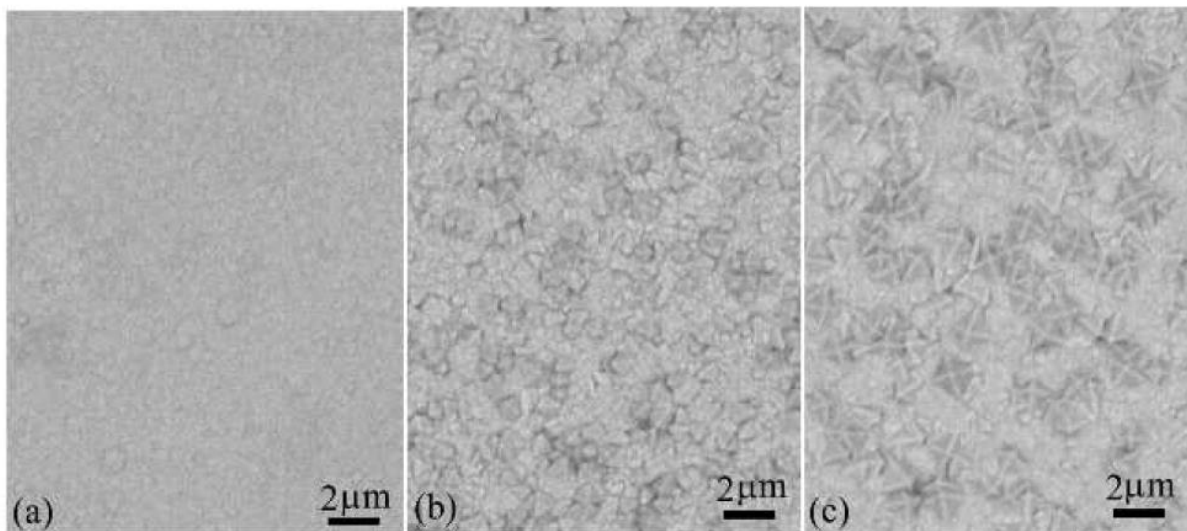


Figure 6. SEM images of the gold thin film having a film thickness of (a) 0.95 μm, (b) 1.1 μm, and (c) 1.35 μm. The gold electrodeposits were generated at a solution temperature of 323 K and at a current density of 22.4 mA/cm².

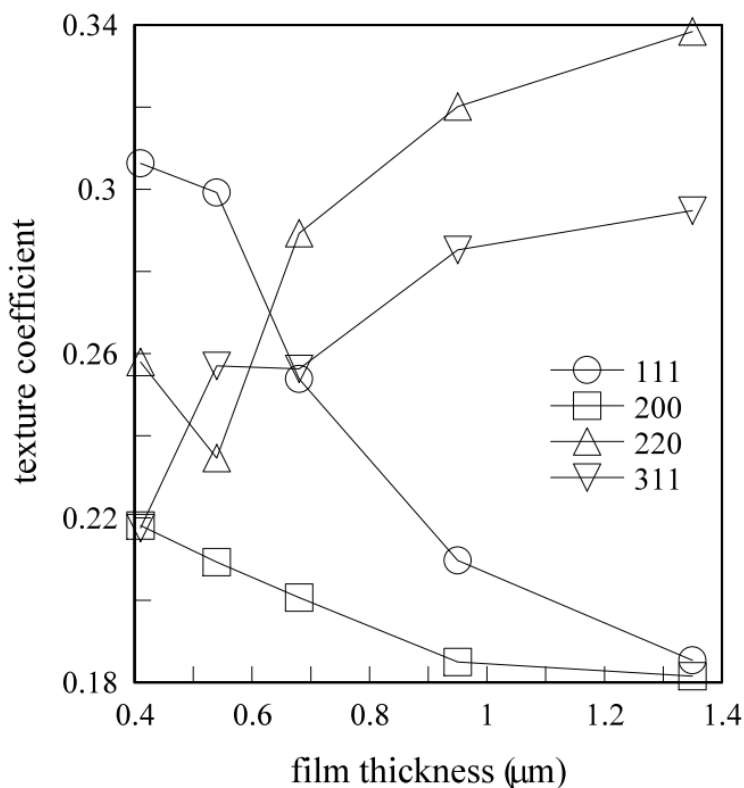


Figure 7. A plot of the texture coefficient vs. the film thickness. The gold thin films were generated at a solution temperature of 323 K, a current density of 22.4 mA/cm².

Figure 7 shows a plot of the texture coefficient vs. the film thickness. The texture change between the (220) plane and the (111) plane occurs at a film thickness of 0.64 μm. The texture change

between the (311) plane and the (111) plane also occurs at a film thickness of $0.7 \mu\text{m}$. The texture change takes place at a thicker film thickness than that at a temperature of 313 K.

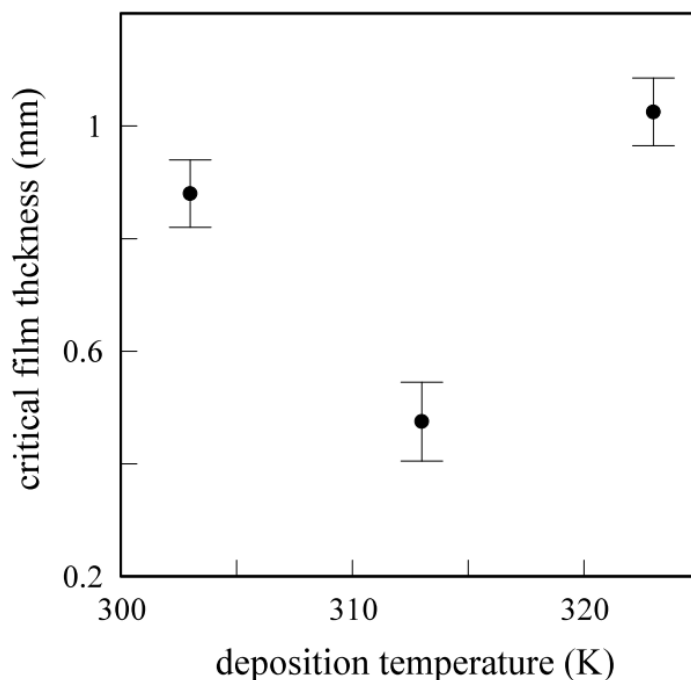


Figure 8. A plot of the critical film thickness vs. the deposition temperature.

The critical film thickness dependent on temperature is summarized in Fig. 8. The critical film thickness does not monotonously decrease with temperature. In electrodeposition, the appearance of the crystallographic plane is more complicated than that in vapor phase epitaxy. The exchange current density and the surface energy depend on not only the crystallographic plane but also temperature. In fact, the texture coefficient of the (220) plane is dependent on temperature as shown in Figs. 3, 5, and 7.

3.2 Internal stress in the gold thin film

Figure 9 shows a plot of the internal stress vs. the film thickness. The gold thin film was generated at a temperature of 303 K. The internal stress decreases with the film thickness and changes from a tensile stress to a compressive one at a film thickness of $0.5 \mu\text{m}$. The internal stress at the critical film thickness of $0.85 \mu\text{m}$ at 303 K becomes -11 MP and the strain in the gold thin film is very small. Hence, the strain energy gradually decreases with the film thickness and has a zero at a film thickness of $0.5 \mu\text{m}$. In the framework of the S-K mode transition, the strain energy increases with the film thickness and the increase in the strain energy causes the S-K transition. However, it may be concluded that the strain in the gold thin film is too small to cause the S-K transition. The proposed theoretical models [23-24] that do not take into consideration the crystallographic plane can not predict the S-K transition in this study.

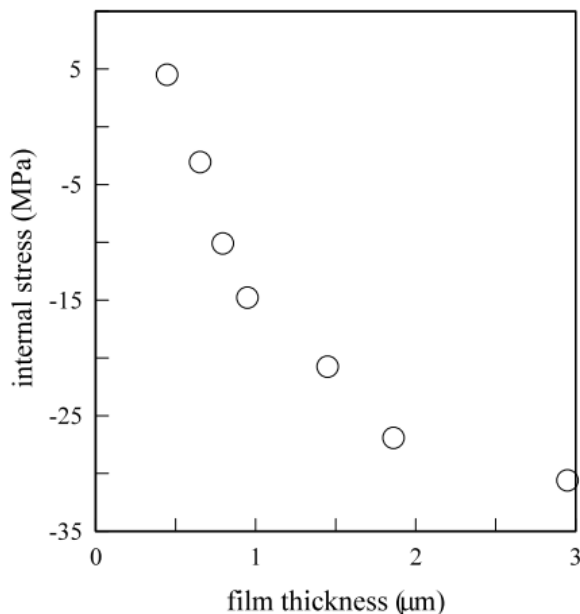


Figure 9. A plot of the internal stress vs. the film thickness. The gold thin film was generated at a temperature of 303 K, a current density of 22.4 mA/cm^2 , and a frequency of 1 MHz.

The competition between the (110) plane and the other planes is related to the S-K transition. The surface energy, edge energy, and entropy are deeply involved with the crystallographic plane. As the (110) and the (311) plane have a large surface energy, the appearance of the pyramid-like electrodeposit with the four (111) planes lessens the total surface energy.

3.3 S-K mode transition for quantum dots

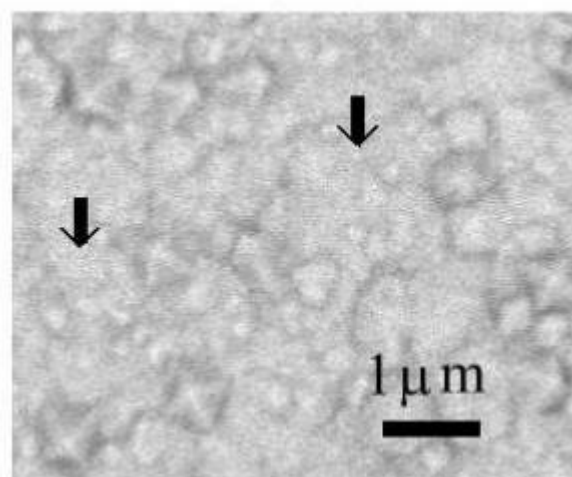


Figure 10. SEM images of the gold thin film having a film thickness of 1.1 μm . The gold electrodeposits were generated at a solution temperature of 323 K and at a current density of 22.4 mA/cm^2 .

Figure 10 shows a SEM image of the pyramid-like electrodeposit generated at the critical film thickness. The arrow shows the pyramid-like electrodeposit having a smaller size than 50 nm, which indicates that it is possible to be a candidate for the generation of the gold quantum dots [25-26]. Owing to a limited spatial resolution of our SEM, it is unclear whether or not the pyramid-like electrodeposit in the order of nanometer is composed of the facet such as the (111) plane.

4. CONCLUSIONS

The S-K mode transition in gold electrodeposition was found. The pyramid-like gold electrodeposit emerged on the smooth gold thin film generated on the ITO glass. The critical film thickness less than 1 μm , which is dependent on temperature, has a minimum. The texture coefficient of the gold thin film determined by XRD reveals that the S-K mode transition occurs when the (110) plane becomes dominant. The SEM image shows that the pyramid-like gold electrodeposit may become a candidate for the quantum dots

References

1. S. Dey and J. Zhao, *J. Phys. Chem. Lett.*, 7 (2016) 2921.
2. D. S. Rahman and S. K. Ghosh, *J. Phys. Chem. C*, 120 (2016) 14906.
3. Y. Volkov, *Biochem. Biophys. Res. Commun.* 468 (2015) 419.
4. L. Sus, Y. Okhremchuk, I. Saldan, O. Kuntiyi, O. Reshetnyak, and S. Korniy, *Mater. Lett.*, 139 (2015) 296.
5. Y. Tu and J. Tersoff, *Phys. Rev. Lett.*, 93 (2004) 216101.
6. A. Baskaran and P. Smereka, *J. Apply. Phys.*, 111 (2012) 044321.
7. A. G. Cullis, D. J. Norris, T. Walther, M. A. Migliorato, and M. Hopkinson, *Phys. Rev. B*, 66 (2002) 081305.
8. T. Walther, A. G. Cullis, D. J. Norris, and M. Hopkinson, *Phys. Rev. Lett.*, 86 (2001) 2381.
9. K. Tai, T. J. Houlahan, Jr., J. G. Eden, and S. J. Dillon, *Sci. Rep.*, 3 (2013) 1.
10. N. Ferralis, R. Maboudian, and C. Carraro, *J. Phys. Chem. C*, 111 (2007) 7508.
11. A. I. de Sá, S. Eugénio, S. Quaresma, C. M. Rangel, and R. Vilar, *Thin Solid Films* 519 (2011) 6278.
12. S. Sobri, S. Roy, D. Aranyi, P. M. Nagy, K. Papp, and E. Kalman, *Surf. Interface Anal.*, 40 (2008) 834.
13. L. P. Bicelli, B. Bozzini, C. Mele, and L. D'Urzo, *Int. J. Electrochem. Sci.*, 3 (2008) 356.
14. M. G-Balcázar¹, R. Ortega¹, F. Castaneda¹, L. G. Arriaga¹, J. L-Garcia, *Int. J. Electrochem. Sci.*, 6 (2011) 4667.
15. E. Sibert, F. Ozanam, F. Maroun, R. J. Behm, and O. M. Magnussen, *Surf. Sci.*, 572 (2004) 115.
16. M. Saito, *Int. J. Electrochem. Sci.*, 11 (2016) 6491.
17. J. J. Kelly, N. Yang, T. Headley, and J. Hachman, *J. Electrochem. Soc.*, 150 (2003) C445.
18. JCPDS-ICDD Card No. 04-0784.
19. M. Kang, H. Lee, T. Kang, and B. Kim, *J. Mater. Sci. Technol.*, 321 (2015) 573.
20. N. E. Singh-Miller and N. Marzari, *Phys. Rev. B*, 80 (2009) 235407.
21. G. J. Brug, M. S-Rehbach, and J. H. Sluyters, *J. Electroanal. Chem.*, 181 (1984) 245.

22. S. Naveenraj, R. V. Mangalaraja, J. J. Wu, A.M. Asiri, and S. Anandan, *Langmuir*, 32 (2016) 11854.
23. K. A. Lozovoy, A. P. Kokhanenko, and A. V. Voitsekhovskii, *Appl. Phys. Lett.*, 109 (2016) 021604.
24. A. Grimm, A. Fissel, E. Bugiel, T. F. Wietler, *Appl. Surf. Sci.*, 370 (2016) 40.
25. X-Y. Yu, J-Y. Liao, K-Q. Qiu, D-B. Kuang, and C-Y. Su, *ACS Nano*, 5 (2011) 9494.
26. R. J. Jam, M. Heurlin, V. Jain, A. Kvennefors, M. Graczyk, I. Maximov, M. T. Borgström, H. Pettersson, and L. Samuelson, *Nano Lett.*, 15 (2015) 134.

© 2017 The Authors. Published by ESG (www.electrochemsci.org). This article is an open access article distributed under the terms and conditions of the Creative Commons Attribution license (<http://creativecommons.org/licenses/by/4.0/>).